HHS Public Access

Author manuscript

*J Proteome Res*. Author manuscript; available in PMC 2017 August 01.

Published in final edited form as:

*J Proteome Res*. 2017 April 07; 16(4): 1506–1514. doi:10.1021/acs.jproteome.6b00905.

# Multiplexed Phosphoproteomic Profiling Using Titanium Dioxide and Immunoaffinity Enrichments Reveals Complementary Phosphorylation Events

**Anthony P. Possemato**[†,§], **Joao A. Paulo**[‡,§], **Daniel Mulhern**[†], **Ailan Guo**[†], **Steven P. Gygi**[‡], and **Sean A. Beausoleil**[*,†]

[†]Bluefin Biomedicine, Beverly, Massachusetts 01915, United States

[‡]Department of Cell Biology, Harvard Medical School, Boston, Massachusetts 02115, United States

## Abstract

A comprehensive view of protein phosphorylation remains an unmet challenge in the field of cell biology. Mass spectrometry-based proteomics is one of the most promising approaches for identifying thousands of phosphorylation events in a single experiment, yet the full breadth of the phosphoproteome has yet to be elucidated. In this article, we examined the complementarity of two methods for phosphopeptide enrichment based on either titanium dioxide ($TiO_2$) enrichment or phosphorylation motif-specific immunoaffinity precipitation (IAP) with four different antibodies. Each method identified nearly 2000 phosphoproteins. However, distinct populations of phosphopeptides were observed. Despite quantifying over 10 000 unique phosphorylation events using $TiO_2$ and over 3900 with IAP, less than 5% of the sites were in common. Agreeing with published literature, the ratio of pS:pT:pY phosphorylation for the $TiO_2$-enriched data set approximated 90:10:<1. In contrast, that ratio for the combined IAP data sets was 51:29:20. These differences not only suggest the complementarity between multiple enrichment methods but also emphasize their collective importance in obtaining a comprehensive view of the phosphoproteome.

## Graphical Abstract

[*]Corresponding Author: sbeausoleil@bluefinbiomed.com.

[§]**Author Contributions**

A.P.P. and J.A.P. contributed equally to this work.

**ORCID**

Joao A. Paulo: 0000-0002-4291-413X

Sean A. Beausoleil: 0000-0002-3356-4641

**Notes**

The authors declare no competing financial interest.

Supporting Information

The Supporting Information is available free of charge on the ACS Publications website at DOI: 10.1021/acs.jproteo-me.6b00905. Analysis of phosphopeptide enrichment; kinases identified by $TiO_2$ and IAP enrichments; and sequence logos for phosphorylation sites (PDF)

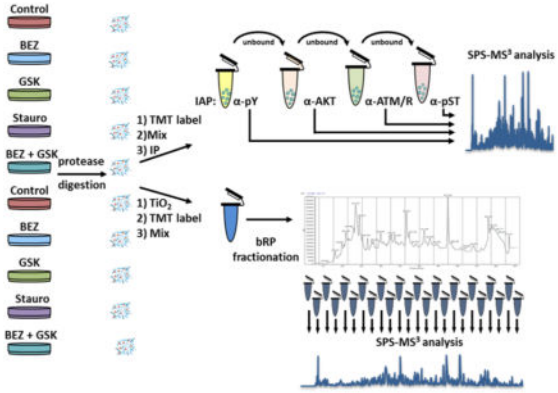


**Keywords**

SPS-MS$^3$; TMT; phosphoproteome; pY; titanium dioxide; phosphoproteomics; $TiO_2$

## INTRODUCTION

The study of protein phosphorylation and its implications in cellular regulation and disease progression has persisted for several decades, yet it remains a very active area of research. With mass spectrometry-based phosphoproteomics becoming increasingly routine, the number of nonredundant phosphorylation sites and phosphoproteins in PhosphoSitePlus has increased to nearly 250 000 and 19 600, respectively, in the last 10 years.[1–3] Growth in this field has been driven largely by improvements in enrichment strategies, specifically in the segregation of phosphopeptides from their unmodified counterparts and advancements in instrumentation.[4–7]

Several phosphopeptide enrichment strategies have been applied successfully to mass spectrometry-based investigations. The generation of motif-specific antibodies recognizing phosphorylated residues has proven to be both challenging and successful, as with phosphotyrosine (pTyr).[8–10] In addition to motif-specific antibodies, phosphopeptides are enriched by their selective interaction with metals in the form of chelated metal ions[11–16] or metal oxides.[16] Each of these strategies has specific advantages and disadvantages concerning enrichment specificity and phosphopeptide recovery, in addition to cost and duration of the procedure. For example, when comparing IMAC and $TiO_2$ enrichments, phosphopeptides unique to IMAC enrichment showed a higher percentage of multi-phosphopeptides as well as a higher percentage of longer, basic, and hydrophilic phosphopeptides. As such, it follows that the IMAC and $TiO_2$ procedures enriched phosphopeptides with different motifs.[17] In the case of IMAC, a chelated metal ion able to bind phosphopeptides noncovalently is attached to a matrix, such as nitrilotriacetate or iminodiacetate. A caveat of conventional IMAC materials is the relatively low enrichment specificity as nonphosphorylated peptides with multiply acidic residues tend to show strong nonspecific binding. For $TiO_2$, negatively chelated phosphopeptides interact with metal in the form of covalent oxides. The interaction mechanisms are thought to be both ion exchange and Lewis acid/base interactions, which result in relatively higher specificity.[18]

Although various strategies are available, obtaining a comprehensive view of protein phosphorylation remains a challenge. As instrumentation matures and enrichment strategies become more efficient, large-scale phosphoproteomic data sets have been shown to reach thousands of nonredundant sites in a single experiment.[19,20] Phosphopeptide enrichment strategies provide researchers with proteome-wide access to phosphorylation events; however, extracting biological relevance remains difficult. With currently available strategies, questions persist as to which phosphorylation events have been missed, thereby resulting in an unclear view of the biological significance of the data. In this article, we explored two commonly used phosphopeptide enrichment strategies that yield distinct populations of phosphorylation sites from the same amount of starting material. Using H460 cell lysate, we identified over 7800 unique, localized phosphorylation events with titanium dioxide ($TiO_2$) followed by basic reversed-phase fractionation. In addition, we identified over 2400 sites with four different commercially available phosphorylation motif-specific antibodies. Remarkably, despite identifying nearly 8000 sites by $TiO_2$, the total overlap of unique sites with the IAP was less than 5%.

We conducted our analysis using different treatment conditions to understand better the inconsistent nature of phosphorylation enrichment and to determine what population of phosphorylated peptides is captured by each strategy. We treated H460 lung cancer cells with three different kinase inhibitors, BEZ-235, GSK1120212, and staurosporine, and measured their response to the inhibitors. We hypothesized that these three compounds would disrupt diverse signaling pathways and result in a wide spectrum of phosphorylation events. By using an isobaric labeling workflow, we combined the five conditions in duplicate into a single multiplexed experiment using tandem mass tags (TMT10-plex), thereby permitting the comparison of relative phosphorylation levels across samples. The data described here provide further insight into the strengths of complementary phosphorylation enrichment methods and emphasize the importance of considering innovative strategies to establish a comprehensive view of the phosphoproteome.

## METHODS

### Materials

Tandem mass tag (TMT) isobaric reagents were from ThermoFisher Scientific (Waltham, MA). Water and organic solvents were from J.T. Baker (Center Valley, PA). Dulbecco's modified Eagle's medium (DMEM) supplemented with 10% fetal bovine serum (FBS) was from LifeTechnologies (Waltham, MA). Unless otherwise noted, all other chemicals were from Sigma (St. Louis, MO). Titanosphere $TiO_2$ 5 $\mu$m particles were from GL Biosciences, (Tokyo, Japan). We used the following commercial antibodies from Cell Signaling Technology: $\alpha$-pY (p-Tyr 1000, cat. no. 8954), $\alpha$-pAKT/AMPK (cat. no. 9614), $\alpha$-pATM/R (cat. no. 6966), and $\alpha$-pST (cat. no. TBD).

### Lysis, Digestion, and Preparation for Mass Spectrometric Analysis

H460 cells were cultured in RPMI 1640 supplemented with 10% fetal bovine serum and 0.5% penicillin/streptomycin at 37 °C in 5% $CO_2$. Cells were briefly trypsinized with 0.15% trypsin. The cells were collected and washed with PBS before snap freezing in a dry ice bath

and storing at −80 °C. Cell pellets were lysed using 10 mL of lysis buffer (8 M urea, 20 mM HEPES pH 8, phosphatase inhibitors (1 mM β-glycerophosphate, 1 mM sodium orthovanadate)) and sonicated (three times for 15 s bursts, resting on ice between sonication steps). Samples were then centrifuged at 12 000 rpm for 5 min at 4 °C, and supernatants were transferred into new microcentrifuge tubes. Samples were reduced by adding 1/10th the total sample volume of 45 mM DTT followed by a 30 min incubation at 55 °C. Lysates were then allowed to cool before alkylation in the dark at room temperature with the addition of 1/10th the total sample volume of 100 mM iodoacetamide. Samples were then diluted 4-fold with 20 mM HEPES pH 8. Protein content was estimated using a Bradford assay. Samples were then digested overnight with trypsin at an enzyme to protein ratio of 1:100 at room temperature with slight sample rocking. After digestion, samples were purified over SepPak C18 columns and the eluted peptides were divided into 5 mg aliquots and lyophilized. For the IAP, 1 mg of tryptic peptides per each of the 10 channels was labeled and then combined before serial IAP enrichments. $TiO_2$ enrichments were performed on 10 mg of starting material per treatment condition; then, enriched peptides were split into technical replicates before TMT labeling.

## Cell Line Treatments

The lung cancer cell line H460 was chosen for inhibitor treatment experiments. In determining the best possible system for this study, we chose a panel of four lung cancer cell lines: H1299, H1666, H23, and H460. Each cell line was treated with two different concentrations of each drug (0.1 or 1 μM BEZ-235, 0.1 or 1 μM GSK1120212, and 0.1 or 1 μM staurosporine independently, as well as a combination of 0.1 μM BEZ-235 and 1 μM GSK1120212). The treatment was performed for 3 and 24 h. For the final experimental sample, H460 cells were treated for 3 h with 1 μM BEZ-235, 1 μM GSK1120212, a combination of these two (1 μM GSK1120212 + 0.1 μM BEZ-235), or 1 μM staurosporine, as these conditions demonstrated a response to treatment while simultaneously minimizing cell death. After treatment, plates were washed with cold sterile PBS before harvesting in lysis buffer.

## Cell Growth Inhibition Assay

CellTiter 96 Aqueous One solution cell proliferation assay (Promega) was performed according to the manufacturer's instructions. Briefly, 1000–5000 cells were seeded onto flat-bottomed 96-well plates and grown in complete medium with 10% FBS. After 24 h, the cell medium was changed to 100 μL complete growth medium with 10% FBS containing various concentrations of kinase inhibitors, and the cells were incubated for an additional 72 h. Each drug concentration was applied to cells in triplicate wells. At the end of the incubation, 20 μL of CellTiter 96 Aqueous was added. One solution was added to each well, and the plate was incubated for 1–4 h. Absorbance was read at 490 nm using a Titan Multiskan Ascent microplate reader (Titertek Instrument). Growth inhibition was expressed as the mean ± standard deviation of the percentage of absorbance from treated cells versus untreated cells. The assay was repeated at least three times.

### Immunoaffinity Precipitation with Motif Antibodies

The appropriate amount of protein A beads (Roche) was washed three times with PBS by centrifugation at 5000 rpm for 30 s, and the pellet was resuspended again with PBS. After the final wash, the PBS was aspirated and the appropriate amount of antibody (100 $\mu$g of pY and pATM/R and 160 $\mu$g of pAKT/AMPK and pST) was added to the resin. Beads were then incubated with antibody and rotated overnight at 4 °C. After the overnight incubation, beads were washed again three times with PBS and added to the peptides.

For these experiments, we used pY-, pAKT/AMPK-, pATM/R-, and pST-directed antibodies sequentially in this order for our immunoprecipitations. Antibodies were added to the lysate, rotated for a minimum of 3 h at 4 °C, and then centrifuged at 5000 rpm for 30 s to collect the immunoprecipitated peptides. The supernatant was passed on to the next antibody until all of the IAPs had been completed (Figure 1). After the final IAP, beads were washed three times with IAP buffer and twice with ultrapure water, and peptides were eluted from the beads in two steps with 15 min incubations in 0.15% TFA. Elutions for each antibody were combined and purified over a C18 StageTip before being subjected to mass spectrometry analysis.

### Titanium Dioxide ($TiO_2$) Enrichment

$TiO_2$ enrichment was performed on 10 mg of starting material for each treatment based on a protocol by Kettenbach and Gerber.[16] $TiO_2$ resin was resuspended in 100% ACN. The appropriate amount of beads (400 $\mu$g beads/100 $\mu$g peptides) was washed three times with binding solution (2 M lactic acid/50% ACN). The resin was then resuspended in 1 mL of binding solution and added to 10 mg of dried H460 peptides. The sample was then vortexed for 1 h at room temperature. The resin was then washed twice with 500 $\mu$L of the binding solution followed by three washes with 500 $\mu$L of 50% ACN/0.1% TFA. After the final wash, peptides were eluted from the resin in two steps with 500 $\mu$L of 50 mM $KH_2PO_4$ (adjusted to pH 10 with ammonium hydroxide). Elutions were combined and quenched with 500 $\mu$L of 50% ACN/5% formic acid, dried, and desalted over a 50 mg C18 SepPak.

### TMT Labeling of H460 Proteolyzed Lysates

For the IAP arm of the experiment, 1 mg of starting material was labeled for each channel. Peptides were resuspended in 500 $\mu$L of 200 mM HEPES, pH 8.5. TMT reagents were resuspended in 100% ACN, and 2 mg was then added to each sample. Samples were then vortexed and incubated at room temperature for 1 h. After incubation, samples were quenched with hydroxylamine and again incubated at room temperature for 15 min. After quenching, a small amount of each channel was combined, dried, desalted over a StageTip, and analyzed for labeling and mixing.

Samples enriched by $TiO_2$ were labeled after enrichment. These samples were resuspended in 100 $\mu$L of 200 mM HEPES, pH 8.5, and 200 $\mu$g of TMT reagent (resuspended in 100% ACN) was added to each sample. The TMT labels used for each sample were as follows: 126, control; 127N, BEZ-235 only; 127C, GSK1120212 only; 128N, staurosporine only; 128C, 1 $\mu$M GSK1120212/0.1 $\mu$M BEZ-235; 129N, control; 129C, BEZ-325 only; 130N, GSK1120212 only; 130C, staurosporine only; and 131, 1 $\mu$M GSK1120212/0.1 $\mu$M BEZ-325. After the 1 h incubation at room temperature, the samples were quenched with

hydroxylamine and a small fraction of each was combined again for label check to ensure 1:1 mixing across all channels. All samples were also searched again with TMT as a variable modification to determine sample labeling. In both cases, $TiO_2$ and IAP identified peptides demonstrated that ~82% of the N-terminus and ~95% of lysine residues were TMT labeled. Protein precipitation prior to labeling will increase labeling efficiency to >99% (unpublished observation).

### Basic pH Reversed-Phase Liquid Chromatography

Samples were resuspended in 200 $\mu$L of bRP buffer A (10 mM $NH_4HCO_2$, pH10/5% ACN) and separated on a Zorbax Extended C18 bRP column (2.1 × 150 mm, 5 $\mu$m, no. 773700-902, Agilent) using a gradient of 10–40% bRP buffer B (10 mM $NH_4HCO_2$, pH10/90% ACN) over 50 min at a flow rate of 200 $\mu$L/min. A total of 96 fractions were collected before further concatenation into 24 final fractions.[21] Each fraction was then dried and desalted over a C18 StageTip prior to analysis by mass spectrometry.

### LC–MS/MS Analysis

All samples were analyzed on an Orbitrap Fusion mass spectrometer (Thermo Fisher Scientific, San Jose, CA) coupled with a Proxeon EASY-nLC 1000 liquid chromatography (LC) pump (Thermo Fisher Scientific). Peptides were separated on a 100 $\mu$m inner diameter microcapillary column packed with 0.5 cm of Magic C4 resin (5 $\mu$m, 100 Å, Michrom Bioresources) followed by 35 cm of Accucore C18 resin (2.6 $\mu$m, 150 Å, ThermoFisher). For each analysis, we loaded approximately 1 $\mu$g onto the column. Peptides were separated using either a 2 or 3 h gradient of 6–30% acetonitrile in 0.125% formic acid with a flow rate of 150 nL/min. Each analysis used an $MS^3$-based TMT method,[22,23] which has been shown to reduce ion interference compared to $MS^2$ quantification.[24] The scan sequence began with an $MS^1$ spectrum (Orbitrap analysis, resolution 60 000, 300–1500 Th, automatic gain control (AGC) target $1 \times 10^6$, maximum injection time 150 ms). The top 10 precursors were then selected for $MS^2/MS^3$ analysis. $MS^2$ analysis consisted of collision-induced dissociation (CID), quadrupole ion trap analysis, automatic gain control (AGC) $2 \times 10^3$, NCE (normalized collision energy) 35, *q*-value 0.25, and maximum injection time 100 ms. Following acquisition of each $MS^2$ spectrum, we collected an $MS^3$ spectrum using our recently described method in which multiple $MS^2$ fragment ions are captured in the $MS^3$ precursor population using isolation waveforms with multiple frequency notches.[23] $MS^3$ precursors were fragmented by HCD and analyzed using the Orbitrap (NCE 50, AGC $1.5 \times 10^5$, maximum injection time 250 ms, isolation specificity 0.8 Th, resolution was 60 000 at 400 Th).

### Data Processing and Analysis

Following data collection, RAW files were processed using Sequest and filtered to 2% FDR at the protein level. Samples were searched using a semitryptic database allowing for a static modification of lysine and N-termini with TMT (229.1629 Da) and carbamidomethylation (57.0215 Da) of cysteine. A variable modification for phosphorylation (79.9663 Da) was allowed on serine, threonine, and tyrosine, along with oxidation (15.9949 Da) of methionine. A regular expression for phosphorylation was used to search the $TiO_2$ data sets while specific motif-oriented expressions were used for the IAPs. Peptide-spectral matching was

performed using linear discriminant analysis (LDA) set to a false discovery rate (FDR) of 2% while considering XCorr, deltaCn, tryptic state, missed cleavages, adjusted ppm, peptide length, peptides/protein, PSMs/protein, corrected protein counts, and charge state.[25,26] Proteins were filtered to a 1% FDR.

Unique identified sites from each method were evaluated using AScore.[27] Overlapping phosphorylation events between the two data sets were determined only for confidently localized sites with a AScore > 13 ($p$-value < 0.05). Phosphorylation site quantitation was performed using the summed intensity of the reporter ions. Sites with a combined signal-to-noise < 50 were excluded. Samples were normalized for equal protein loading by comparing the summed reporter ions across the 10 channels from the test mix runs.

### Phosphorylation Analysis with Defined Search Space

When searching the $TiO_2$ data set, we allowed for phosphorylation at any serine, threonine, or tyrosine residue while restricting the data set to peptides containing at least one phosphorylation site. For the IAPs, the motif antibody has a specific preference for residues at known motifs, allowing for a more defined search space. We forced the search space to contain peptides that were not only phosphorylated but also must contain a specific motif, e.g., [Rx(S/T)].

We applied this approach to the $\alpha$-pY immunoprecipitated samples. In this case, using that motif allowed for better localization but, overall, identified fewer sites because of the restriction. We then applied this technique to the other motif-specific antibody data. In the case of $\alpha$-AKT, again our initial search required a Rxx(S/T) motif. Requiring this motif here not only identified more peptides but also correctly localized more phosphorylation sites. Because of the specificity of the antibodies, using these motifs is advantageous when searching the data, as not only are more peptides identified but also better site localization is achieved.

## RESULTS

### Titanium Dioxide and Immunoaffinity Enriched Phosphopeptides Identified Using Mass Spectrometry-Based Techniques

We designed a TMT-based workflow to compare two phosphopeptide enrichment strategies: $TiO_2$ and IAP (Figure 1). Sequential IAPs were performed on the TMT-labeled mixture. Each IAP was analyzed twice to reduce the stochastic nature inherent to bottom-up proteomics.

Data were collected using $MS^2$-based sequence identification and $MS^3$-based quantification of TMT reporter ions.[22,23] We monitored phosphopeptide enrichment for each method by comparing the total unique phosphopeptides to the total unique peptides identified. For $TiO_2$ fractions, the average phosphopeptide enrichment was ~65% (Figure S1A), whereas enrichments for the IAPs ranged from as low as 9% with $\alpha$-AKT to as high as 37% from the $\alpha$-pST (Figure S1B). The $TiO_2$-enriched sample analysis resulted in a total of 24 LC–$MS^3$ data files, yielding 38 766 phosphopeptides. After performing localization analysis using AScore, 7870 unique phosphorylation sites were identified, mapping to 1804 proteins. The

total time for data collection of the $TiO_2$ data set was 48 h. Separately, samples from the IAPs, were analyzed using a similar strategy. For these enrichments, we analyzed eight samples (each of the four antibodies in duplicate), resulting in 13 025 total phosphopeptides. After performing localization analysis using AScore,[27] a total of 2466 unique phosphorylation events were identified, which mapped to 1432 proteins. The data collection for the IAP samples totaled 24 h.

In addition, we compared peptide overlap among $TiO_2$ fractions and the duplicate IAPs. The peptide overlap among $TiO_2$ fractions reached no higher than 28% (between chromatographically adjacent pooled samples) with most fractions having less than 10% overlap. The low overlap among fractions increased our analytical depth. As expected, unfractionated replicate IAPs had much higher overlap, over 55%. The overlap observed in our experiments were in line with those previously reported for $TiO_2$ fractionation and IAPs. [28]

## Different Enrichment Strategies Reveal Strong Overlap at the Phosphoprotein Level

Each approach resulted in the identification of nearly 2000 unique phosphoproteins, with an overlap of approximately 40% (Figure 2A). Gene ontology analysis revealed that many of the overlapping proteins were classified in common structural, cell cycle, transcription, and RNA processing subfamilies (Figure 2B). However, the nonoverlapping proteins helped reveal how the two approaches differed. For example, although the number of kinases independently identified between the two approaches was comparable, slightly more were identified with IAP (Figure S2A). More specifically, IAP and $TiO_2$ identified a total of 119 and 96 kinases, respectively, with an overlap of 53 (Figure S2B). Tyrosine kinases were of interest because of their implication in cancer and its treatment. Our data showed, not surprisingly, that $\alpha$-pY IAP identified 7 of the 8 tyrosine kinases that were enriched by $TiO_2$. In addition, the $\alpha$-pY IAP identified another 16 tyrosine kinases that were not observed in the $TiO_2$ enrichment analysis (Figure S2C). Although the overlap is strong at the phosphoprotein level, differences in enrichment are apparent among the strategies investigated.

## Distribution of Phosphorylated Residues Varies with Enrichmental Approach

To evaluate the phosphorylation events quantified in each data set, we calculated the distribution of pS, pT, and pY sites observed in each data set relative to the total number of observed phosphopeptides. The literature suggests that the ratio of pS:pT:pY phosphorylation within a cell is 90:10:<1.[29] This ratio matches closely with that observed in our $TiO_2$ data set (Figure 3A). In addition, we explored the IAP data as a single data set and for each antibody individually. Surprising, when the IAP data was combined, the observed pS:pT:pY ratio was 51:29:20 (Figure 3A). We also examined the IAP data individually. As expected, when surveying all phosphopeptides identified by IAP, $\alpha$-pY yielded ~90% of the total peptides with a phosphorylated tyrosine. While the $\alpha$-ATM/R IAP showed a similar phosphorylation site distribution as that with $TiO_2$, the other two antibodies behaved differently. For the $\alpha$-AKT IAP, we observed a shift in the number of pT-containing peptides. This trend was even stronger for the $\alpha$-pST IAP, in which the number of identified pT-containing peptides was over 50% (Figure 3B). Overall, we observed differences in the

relative proportion of phosphorylated serine, threonine, and tyrosine residues with respect to the enrichment method.

## The Phosphopeptide Enrichment Strategies Were Complementary

We used two different approaches to evaluate the overlap of each enrichment strategy. First, we took a conservative approach by comparing only the phosphopeptide backbones stripped of all post-translational modifications (PTMs) in each data set. Second, we considered only unique sites localized with an AScore > 13 ($p$-value < 0.05).

We compared nonredundant PTM-stripped phosphopeptides among each IAP enrichment. The IAPs demonstrated very little overlap, which was expected as each antibody was directed to a specific peptide motif (Figure 4A). We then compared the total nonredundant stripped phosphopeptides identified in all IAPs ($n = 8$) to the nonredundant stripped phosphopeptides from the $TiO_2$-enriched data set. A total of 8947 nonredundant peptides were identified in the $TiO_2$ data set, of which only 852 (9.5%) were in common with those peptides identified in the IAPs (Figure 4B).

We extended our analysis to consider only localized phosphorylation events. For phosphorylation events with a peptide localization score > 13 ($p$-value < 0.05), we found that the $TiO_2$ data set yielded 7875 sites and the IAP data set yielded 2466 sites. The overlap of localized sites was 431, less than 5% of the total sites (Table 1). If we examined the data separately by phosphorylated residue, then the largest overlap was among pS-containing peptides, followed by pT-containing peptides, with pY-containing peptides having the least overlap among enrichment methods.

In addition, we compared our data to the recently published ultradeep data set from Sharma et al.[19] This analysis collected 20 times more spectra than our experiment, acquiring nearly 10 million MS/MS scans over approximately 17 days. With such analytical depth, we anticipated their overlap with our data set to be quite high. We first compared all observed sites, independent of site localization. While Sharma et al. observed over 50 000 unique phosphorylation events, our $TiO_2$ data set was only ~50% represented therein and our IAP data, only ~33%. Similar percentages in overlap were observed when comparing confidently assigned sites. This comparison supports the argument that the degree of phosphorylation within a given system is so broad that no single approach is truly comprehensive.

## Quantitation of Phosphorylation Sites Revealed Significant Downregulation upon Drug Treatments

We quantified a total of 4611 confidently assigned unique phosphorylation sites using $TiO_2$ and 1848 with IAP. For each enrichment method, we determined if statistical differences existed between the two groups (control versus inhibitor-treated cells). We observed significant downregulation of phosphorylation events upon drug treatment across all inhibitors for peptides enriched with either the $TiO_2$ or IAP enrichment strategy. In most cases, over 50% of the sites identified for a particular treatment were downregulated, with one case ($TiO_2$ enrichment of GSK1120212-treated cells) in which greater than 80% were downregulated (Figure 5A). Both enrichment methods resulted in an overlap of nearly 40% for phosphoproteins with inhibited phosphorylation (Figure 5B). However, focusing on the

specific phosphorylation events inhibited, the overlap between the two methods was consistently less than 10% for each treatment (Figure 5C). These data again emphasize the complementarity among enrichment methods.

### Downregulated Sites Revealed Over-Represented Motifs

Segregating the downregulated sites by treatment and method revealed differences among identified phosphorylation residues. While the $TiO_2$-enriched data set was dominated by serine phosphorylation (~90% of the phosphorylated events for each treatment), this value decreased to ~50% for the IAPs (Figure 6). We investigated further downregulated sites to determine how the two phosphopeptide enrichment methods compared using Motif X[30,31] analysis.

While several of the more common serine-directed motifs were similar between methods, namely, SP and RxxS, several were specific to only one method. In the case of the $TiO_2$ data set, acidic residues C-terminal to the site of phosphorylation dominated the data. This preference had been reported previously and was not specific to this data set but is, rather, a validation thereof.[13] For the IAPs, the motif SQ appeared in all IAP data sets, but it was not enriched in the $TiO_2$ data set (Figure S3). This example illustrated how the IAPs can enrich unique, potentially low abundance peptides. Because of the limited number of changing pT-directed phosphorylation events in the $TiO_2$ data, the only enriched motif for all drug treatments was TP. The IAPs, while still dominated by TP, returned in some cases as many as seven different over-represented motifs (Figure S3). At this level, a more comprehensive view of the phosphorylation landscape was achieved via complementary phosphopeptide enrichment methods.

## DISCUSSION

While methods to enrich phosphopeptides for analysis by LC–MS/MS have improved over the past decade, questions remain as to the depth and coverage of the phosphoproteome. Typically, 10 000 or more phosphorylation events are observed in a single experiment.[32–34] However, these may represent only a small portion of all phosphorylation events, as evidenced by the low degree of overlap among studies and the limited identification of phosphotyrosine-containing peptides. In this article, we studied phosphorylation in H460 cells under five different conditions using a multiplexed experimental approach. Phosphopeptide enrichment was performed using either $TiO_2$ followed by basic pH reversed-phase fractionation or serial IAPs using four different phosphorylation motif-specific antibodies.

First, we note that the enriched GO terms for phosphorylated proteins for either method are broad in scope and general in nature. Many proteins were classified as having typical cellular and metabolic processes and with functions in cellular component organization and biogenesis.[35–37] No discernible difference was observed when comparing unique proteins identified between methods when using this strategy. As such, each method may be preferentially sampling the most abundant peptides in the sample, as expected when using a bottom-up proteomics approach.

Even with the overlap seen at the protein level and the identification of nearly 14 000 unique phosphorylation events, less than 700 of these sites were identified in both data sets. The combination of the specificity in sequence recognition, based on the antibody–antigen design, and their inherent preference for threonine may compensate for the difference between the methods. While $TiO_2$ enrichment still provides a comparable number of pT sites, 1600, this enrichment is limited by the overwhelming abundance of pS (~9000 sites). Similar to the study of tyrosine phosphorylation (pY), to achieve a higher enrichment specifically of pT-containing peptides, antibody enrichment methods appear advantageous, if not necessary.

When comparing the enrichment between methods of sites that are inhibited upon treatment, again the pS:pT:pY distributions follow the classic 90:10:<1 rule for $TiO_2$. However, enrichment by IAP collectively resulted in a 54:29:20 distribution. We observed significant differences in the number of phosphorylation events changing upon treatment between the two methods. The number of unique sites downregulated in the $TiO_2$ data sets ranged from ~1500 to ~3000 (i.e., ~50% to ~90%) of the quantified sites. In contrast, a range of just over 300 to over 1200 phosphorylation events enriched via IAP were downregulated. Despite not seeming as comprehensive as $TiO_2$, the number of downregulated sites for IAPs accounted for as much as 80% of the quantified phosphorylation events.

The order of the labeling and enrichment strategies (labeling first and then enriching for IAP and vice versa for $TiO_2$) were designed to balance reproducibility and cost. Ideally, labeling the samples first and then enriching would be most efficient and reproducible as all subsequent steps in the procedure following labeling would be performed on a combined sample. Such a scenario thereby limits random errors on one or a few samples which could result in skewed values among different treatments. This reasoning accounted for the up-front TMT labeling in the IAP experiments. For $TiO_2$ enrichment, 10 mg of peptide would require TMT if labeling was to be performed before enrichment. Currently, the cost of such would be prohibitive, and the best balance between reproducibility and cost would be to enrich before labeling for the $TiO_2$ strategy. As the cost of reagents decreases, future studies may be designed to investigate whether the findings herein are dependent on the different orders of enrichment and labeling.

In this article, we observed that using $TiO_2$ as a phosphopeptide enrichment strategy results in the expected distribution of phosphorylation across serine, threonine, and tyrosine residues. In contrast, phosphorylation motif-dependent IAP enrichment yields a much different distribution, potentially due to the specificity of the reagents. As a result, distinct groups of phosphorylation sites are observed. When compared to other published data sets using $TiO_2$ enrichment, this observation holds, suggesting that no single enrichment method can comprehensively cover all phosphorylation events in the cell. As motif-specific antibodies are commonly used to isolate tyrosine-phosphorylated peptides for LC–MS/MS analysis,[8] our data illustrate that threonine-phosphorylated peptide enrichment may also benefit from IAP.

In conclusion, understanding the strengths and weaknesses of novel and incrementally modified enrichment strategies is imperative to achieving a comprehensive map of the

phosphoproteome. While the $TiO_2$ enrichment approach is widely accepted, inherent limitations prevent this and similar methods from rendering a complete atlas of phosphorylation events. As such, IAPs may provide insight especially into populations of pT- and pY-containing peptides, which are relatively under-represented in $TiO_2$ enrichments.[38] Future experiments may use sequential or parallel enrichments using various combinations of the strategies outlined herein to provide a more inclusive profile of the phosphoproteome. Moreover, other enrichment strategies using IMAC, ion exchange (SCX or SAX), hydrophilic interactions (HILIC or ERLIC), or a combination thereof may be compared with the $TiO_2$ and IAP methods described here. The benefits and caveats of each method must be thoroughly assessed to determine which can best address the underlying biological question. Currently, no single all-encompassing phosphopeptide enrichment approach is available, and as such, directed strategies, knowing their limitations, may be the most appropriate method of choice.

## Supplementary Material

Refer to Web version on PubMed Central for supplementary material.

## Acknowledgments

This work was funded in part by NIH/NIDDK grant K01 DK098285 (J.A.P.).

## References

1. Hornbeck PV, Chabra I, Kornhauser JM, Skrzypek E, Zhang B. PhosphoSite: A bioinformatics resource dedicated to physiological protein phosphorylation. Proteomics. 2004; 4(6):1551–61. [PubMed: 15174125]
2. Hornbeck PV, Zhang B, Murray B, Kornhauser JM, Latham V, Skrzypek E. PhosphoSitePlus, 2014: mutations, PTMs and recalibrations. Nucleic Acids Res. 2015; 43(D1):D512–20. [PubMed: 25514926]
3. Hornbeck P, Kornhauser J, Tkachev S, Zhang B, Skrzypek E, Murray B, Latham V, Sullivan M. PhosphoSitePlus: a comprehensive resource for investigating the structure and function of experimentally determined post-translational modifications in man and mouse. Nucleic Acids Res. 2012; 40(D1):D261–70. [PubMed: 22135298]
4. Rosenqvist H, Ye J, Jensen ON. Analytical strategies in mass spectrometry-based phosphoproteomics. Methods Mol Biol. 2011; 753:183–213. [PubMed: 21604124]
5. Thingholm TE, Jensen ON, Larsen MR. Analytical strategies for phosphoproteomics. Proteomics. 2009; 9(6):1451–68. [PubMed: 19235172]
6. Solari FA, Dell'Aica M, Sickmann A, Zahedi RP. Why phosphoproteomics is still a challenge. Mol BioSyst. 2015; 11(6):1487–93. [PubMed: 25800119]
7. Junger MA, Aebersold R. Mass spectrometry-driven phosphoproteomics: patterning the systems biology mosaic. Wiley Interdiscip Rev Dev Biol. 2014; 3(1):83–112. [PubMed: 24902836]
8. Rush J, Moritz A, Lee KA, Guo A, Goss VL, Spek EJ, Zhang H, Zha XM, Polakiewicz RD, Comb MJ. Immunoaffinity profiling of tyrosine phosphorylation in cancer cells. Nat Biotechnol. 2005; 23(1):94–101. [PubMed: 15592455]
9. Moritz A, Li Y, Guo A, Villen J, Wang Y, MacNeill J, Kornhauser J, Sprott K, Zhou J, Possemato A, Ren JM, Hornbeck P, Cantley LC, Gygi SP, Rush J, Comb MJ. Akt-RSK-S6 kinase signaling networks activated by oncogenic receptor tyrosine kinases. Sci Signaling. 2010; 3(136):ra64.
10. Giansanti P, Stokes MP, Silva JC, Scholten A, Heck AJ. Interrogating cAMP-dependent kinase signaling in Jurkat T cells via a protein kinase A targeted immune-precipitation phosphoproteomics approach. Mol Cell Proteomics. 2013; 12(11):3350–9. [PubMed: 23882029]

11. Ficarro SB, McCleland ML, Stukenberg PT, Burke DJ, Ross MM, Shabanowitz J, Hunt DF, White FM. Phosphoproteome analysis by mass spectrometry and its application to Saccharomyces cerevisiae. Nat Biotechnol. 2002; 20(3):301–5. [PubMed: 11875433]
12. Pinkse MW, Uitto PM, Hilhorst MJ, Ooms B, Heck AJ. Selective isolation at the femtomole level of phosphopeptides from proteolytic digests using 2D-NanoLC-ESI-MS/MS and titanium oxide precolumns. Anal Chem. 2004; 76(14):3935–43. [PubMed: 15253627]
13. Bodenmiller B, Mueller LN, Mueller M, Domon B, Aebersold R. Reproducible isolation of distinct, overlapping segments of the phosphoproteome. Nat Methods. 2007; 4(3):231–7. [PubMed: 17293869]
14. Beausoleil SA, Jedrychowski M, Schwartz D, Elias JE, Villen J, Li J, Cohn MA, Cantley LC, Gygi SP. Large-scale characterization of HeLa cell nuclear phosphoproteins. Proc Natl Acad Sci U S A. 2004; 101(33):12130–5. [PubMed: 15302935]
15. Villen J, Gygi SP. The SCX/IMAC enrichment approach for global phosphorylation analysis by mass spectrometry. Nat Protoc. 2008; 3(10):1630–8. [PubMed: 18833199]
16. Kettenbach AN, Gerber SA. Rapid and reproducible single-stage phosphopeptide enrichment of complex peptide mixtures: application to general and phosphotyrosine-specific phosphoproteomics experiments. Anal Chem. 2011; 83(20):7635–44. [PubMed: 21899308]
17. Yue X, Schunter A, Hummon AB. Comparing multistep immobilized metal affinity chromatography and multistep TiO2 methods for phosphopeptide enrichment. Anal Chem. 2015; 87(17):8837–44. [PubMed: 26237447]
18. Leitner A. Enrichment Strategies in Phosphoproteomics. Methods Mol Biol. 2016; 1355:105–21. [PubMed: 26584921]
19. Sharma K, D'Souza RC, Tyanova S, Schaab C, Wisniewski JR, Cox J, Mann M. Ultradeep human phosphoproteome reveals a distinct regulatory nature of Tyr and Ser/Thr-based signaling. Cell Rep. 2014; 8(5):1583–94. [PubMed: 25159151]
20. Zhou H, Di Palma S, Preisinger C, Peng M, Polat AN, Heck AJ, Mohammed S. Toward a comprehensive characterization of a human cancer cell phosphoproteome. J Proteome Res. 2013; 12(1):260–71. [PubMed: 23186163]
21. Paulo JA, O'Connell JD, Everley RA, O'Brien J, Gygi MA, Gygi SP. Quantitative mass spectrometry-based multiplexing compares the abundance of 5000 S. cerevisiae proteins across 10 carbon sources. J Proteomics. 2016; 148:85–93. [PubMed: 27432472]
22. Ting L, Rad R, Gygi SP, Haas W. MS3 eliminates ratio distortion in isobaric multiplexed quantitative proteomics. Nat Methods. 2011; 8(11):937–40. [PubMed: 21963607]
23. McAlister GC, Nusinow DP, Jedrychowski MP, Wuhr M, Huttlin EL, Erickson BK, Rad R, Haas W, Gygi SP. MultiNotch MS3 enables accurate, sensitive, and multiplexed detection of differential expression across cancer cell line proteomes. Anal Chem. 2014; 86(14):7150–8. [PubMed: 24927332]
24. Paulo JA, O'Connell JD, Gygi SP, Triple A. Knockout (TKO) Proteomics Standard for Diagnosing Ion Interference in Isobaric Labeling Experiments. J Am Soc Mass Spectrom. 2016; 27(10):1620–5. [PubMed: 27400695]
25. Elias JE, Gygi SP. Target-decoy search strategy for increased confidence in large-scale protein identifications by mass spectrometry. Nat Methods. 2007; 4(3):207–14. [PubMed: 17327847]
26. Huttlin EL, Jedrychowski MP, Elias JE, Goswami T, Rad R, Beausoleil SA, Villen J, Haas W, Sowa ME, Gygi SP. A tissue-specific atlas of mouse protein phosphorylation and expression. Cell. 2010; 143(7):1174–89. [PubMed: 21183079]
27. Beausoleil SA, Villen J, Gerber SA, Rush J, Gygi SP. A probability-based approach for high-throughput protein phosphorylation analysis and site localization. Nat Biotechnol. 2006; 24(10): 1285–92. [PubMed: 16964243]
28. Guo A, Gu H, Zhou J, Mulhern D, Wang Y, Lee KA, Yang V, Aguiar M, Kornhauser J, Jia X, Ren J, Beausoleil SA, Silva JC, Vemulapalli V, Bedford MT, Comb MJ. Immunoaffinity enrichment and mass spectrometry analysis of protein methylation. Mol Cell Proteomics. 2014; 13(1):372–87. [PubMed: 24129315]
29. Hunter T, Sefton BM. Transforming gene product of Rous sarcoma virus phosphorylates tyrosine. Proc Natl Acad Sci U S A. 1980; 77(3):1311–5. [PubMed: 6246487]

30. Chou MF, Schwartz D. Biological sequence motif discovery using motif-x. Curr Protoc Bioinf. 2011:15–24.

31. Schwartz D, Gygi SP. An iterative statistical approach to the identification of protein phosphorylation motifs from large-scale data sets. Nat Biotechnol. 2005; 23(11):1391–8. [PubMed: 16273072]

32. Paulo JA, Gaun A, Gygi SP. Global Analysis of Protein Expression and Phosphorylation Levels in Nicotine-Treated Pancreatic Stellate Cells. J Proteome Res. 2015; 14(10):4246–56. [PubMed: 26265067]

33. Paulo JA, Gygi SP. A comprehensive proteomic and phosphoproteomic analysis of yeast deletion mutants of 14-3-3 orthologs and associated effects of rapamycin. Proteomics. 2015; 15(2–3):474–86. [PubMed: 25315811]

34. Paulo JA, McAllister FE, Everley RA, Beausoleil SA, Banks AS, Gygi SP. Effects of MEK inhibitors GSK1120212 and PD0325901 in vivo using 10-plex quantitative proteomics and phosphoproteomics. Proteomics. 2015; 15(2–3):462–73. [PubMed: 25195567]

35. Huang DW, Sherman BT, Tan Q, Kir J, Liu D, Bryant D, Guo Y, Stephens R, Baseler MW, Lane HC, Lempicki RA. DAVID Bioinformatics Resources: expanded annotation database and novel algorithms to better extract biology from large gene lists. Nucleic Acids Res. 2007; 35:W169–75. [PubMed: 17576678]

36. Huang DW, Sherman BT, Tan Q, Collins JR, Alvord WG, Roayaei J, Stephens R, Baseler MW, Lane HC, Lempicki RA. The DAVID Gene Functional Classification Tool: a novel biological module-centric algorithm to functionally analyze large gene lists. Genome Biol. 2007; 8(9):R183. [PubMed: 17784955]

37. Huang DW, Sherman BT, Lempicki RA. Systematic and integrative analysis of large gene lists using DAVID bioinformatics resources. Nat Protoc. 2008; 4(1):44–57.

38. Di Palma S, Zoumaro-Djayoon A, Peng M, Post H, Preisinger C, Munoz J, Heck AJ. Finding the same needles in the haystack? A comparison of phosphotyrosine peptides enriched by immunoaffinity precipitation and metal-based affinity chromatography. J Proteomics. 2013; 91:331–7. [PubMed: 23917254]

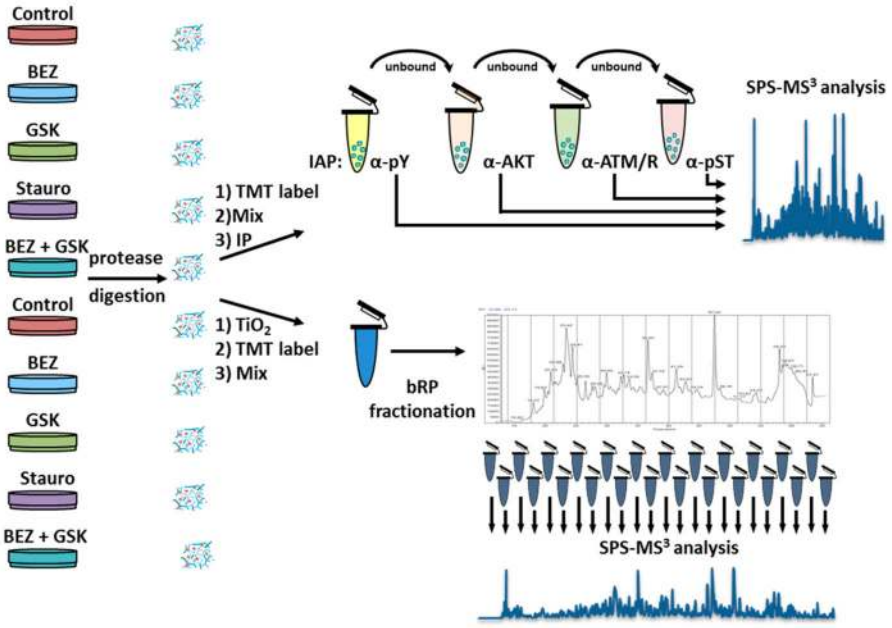


**Figure 1.**

Workflow overview. H460 cells with varying drug treatments were harvested in 8 M urea, reduced, alkylated, and digested with trypsin. The resulting peptides were then divided for both arms of the experiment. The peptides for the IAP arm were pooled, mixed, and subjected to sequential IAPs with $\alpha$-pY, $\alpha$-AKT, $\alpha$-ATM/R, and $\alpha$-pST before SPS-MS$^3$ analysis. Peptides for the $TiO_2$ arm were enriched, labeled, fractionated by bRP, and analyzed using SPS-MS$^3$ analysis.

A)

| Enrichment | Phosphoproteins |
|---|---|
| α-pY | 558 |
| α-ATM/R | 589 |
| α-AKT | 463 |
| α-pST | 1020 |
| $TiO_2$ | 1818 |

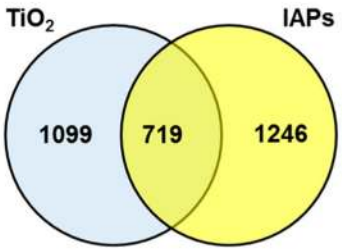


B)

**$TiO_2$ enrichment**

| Term | Count | % | p-value |
|---|---|---|---|
| cellular process | 1205 | 71.3 | 1.40E-34 |
| metabolic process | 853 | 50.4 | 1.10E-09 |
| biological regulation | 826 | 48.8 | 4.90E-08 |
| cellular component organization | 435 | 25.7 | 5.30E-40 |
| cellular component biogenesis | 161 | 9.5 | 1.00E-10 |
| death | 104 | 6.2 | 5.40E-05 |
| multi-organism | 87 | 5.1 | 7.60E-03 |
| viral reproduction | 12 | 0.7 | 8.30E-02 |

**IAP enrichment**

| Term | Count | % | p-value |
|---|---|---|---|
| cellular process | 1304 | 70.9 | 1.10E-33 |
| metabolic process | 930 | 50.6 | 2.00E-10 |
| biological regulation | 871 | 47.4 | 4.20E-05 |
| cellular organization | 454 | 24.7 | 1.80E-36 |
| developmental | 359 | 19.5 | 7.40E-02 |
| cellular component biogenesis | 159 | 8.6 | 1.50E-07 |
| multi-organism | 106 | 5.8 | 5.40E-05 |
| death | 104 | 5.7 | 1.30E-03 |
| viral reproduction | 13 | 0.7 | 7.10E-02 |

**Figure 2.**

Overlap at the phosphoprotein level. (A) Tally of phosphoproteins for each enrichment strategy and Venn diagram of corresponding overlap. (B) Gene ontology (GO) annotation summaries for $TiO_2$ and IAP enrichment strategies.

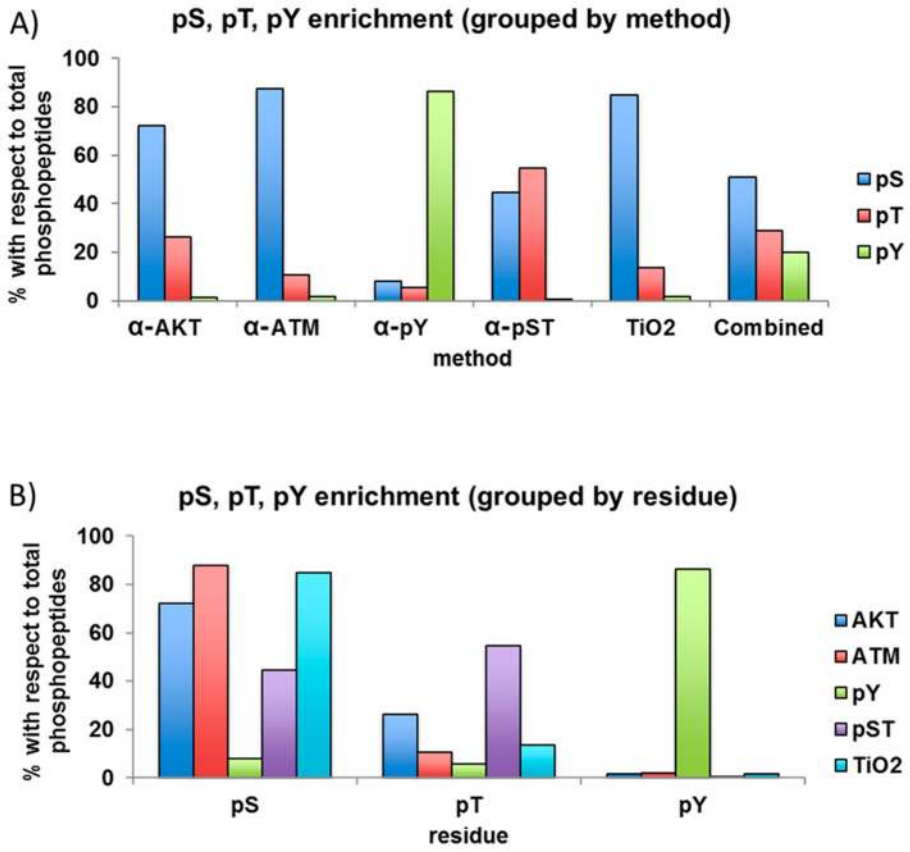


**Figure 3.**

Distribution of phosphorylated residues. The enrichment of each phosphorylated residue with respect to all phosphopeptides is organized by (A) method and (B) amino acid residue.

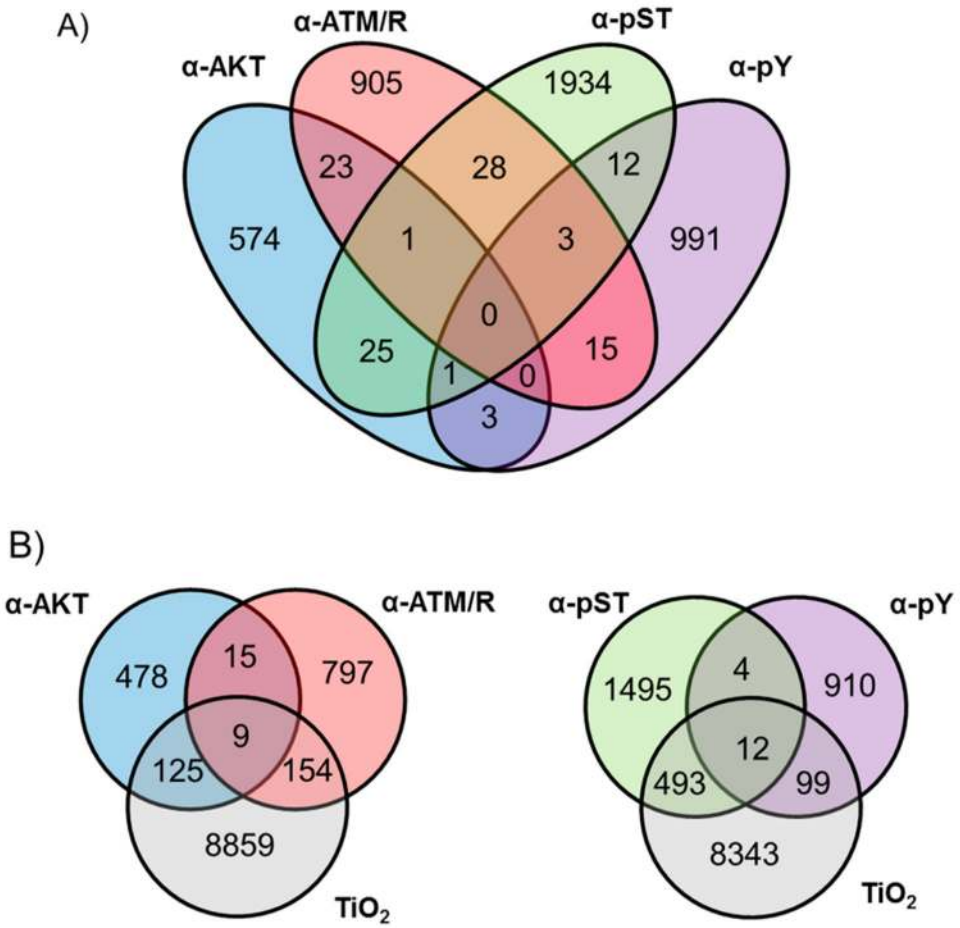


**Figure 4.**

Overlap of the phosphopeptides quantified by each strategy. (A) Venn diagram displaying overlap of the four immunoaffinity precipitation (IAP) strategies. (B) Venn diagrams of two IAP strategies and the $TiO_2$ strategy.

A)

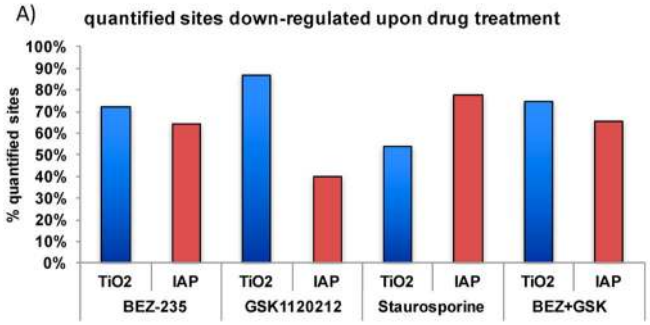


B)

| treatment | phosphoproteins with altered phosphorylation | | |
|---|---|---|---|
| | $TiO_2$ | IAPs | overlap |
| BEZ-235 | 931 | 541 | 227 |
| GSK1120212 | 1339 | 292 | 152 |
| Staurosporine | 833 | 904 | 333 |
| BEZ+GSK | 908 | 482 | 204 |

C)

| treatment | unique phosphorylation sites inhibited | | |
|---|---|---|---|
| | $TiO_2$ | IAPs | overlap |
| BEZ-235 | 1675 | 668 | 52 |
| GSK1120212 | 2956 | 333 | 42 |
| Staurosporine | 1468 | 1241 | 100 |
| BEZ+GSK | 1601 | 568 | 47 |

**Figure 5.**

Effects of kinase inhibitor treatment on phosphorylation sites. (A) Bar chart illustrating the percentage of quantified sites downregulated with respect to treatment. (B) Tally and overlap of proteins with inhibited phosphorylation sites for the $TiO_2$ and IAP enrichments. (C) Tally and overlap of unique phosphorylation sites inhibited by drug treatments for the $TiO_2$ and IAP enrichment strategies.

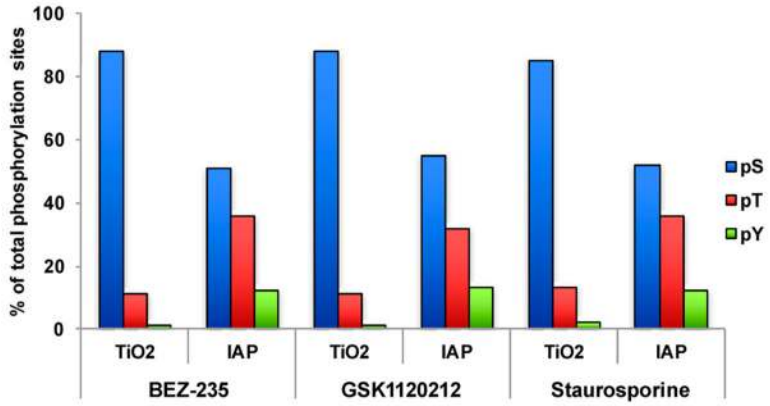


**Figure 6.**

Enrichment of specific phosphorylated residues. The percentage of each phosphorylated residue (pS, pT, and pY) with respect to all phosphorylated sites are illustrated for each drug for both $TiO_2$ and IAP enrichment strategies.

**Table 1**

Phosphorylation Sites Quantified with Both Enrichment Methods

| | number of phosphorylation sites | | |
|---|---|---|---|
| | $TiO_2$ | IAPs | overlap |
| all sites | 10 861 | 3903 | 667 |
| localized sites[a] | 7870 | 2466 | 431 |
| pS | 6753 | 1173 | 278 |
| pT | 973 | 683 | 121 |
| pY | 144 | 610 | 30 |

[a] Phosphorylation sites with AScore > 13 ($p$-value < 0.05).